



A NEW ELECTROCHEMICAL SENSOR FOR DETERMINING ZILEUTON IN PHARMACEUTICAL FORMULATIONS AND SERUM WAS CREATE WITH A NANOCOMPOSITE CARBON PASTE ELECTRODE MODIFIED WITH BIOCL/CUS@SNO2NPS.

Nabil A. Alhemiary^{[a],[b]}

Article History: Received: 28.07.2022

Revised: 28.08.2022

Accepted: 26.09.2022

Abstract: The zileuton was determined utilizing the differential pulse voltammetry (DPV) approach employing a modified molecularly imprinted carbon paste electrode (CPE) containing BiOCl/CuS@SnO₂NPs nanocomposite. The BiOCl/CuS@SnO₂NPs/CPE exhibits a strong and well-defined peak for the oxidation of zileuton at 640 mV in phosphate buffer solution pH = 8. With a linear range of 4-75 μM and a low detection limit of 0.0.7 μM, DPV was used to measure zileuton. BiOCl/CuS@SnO₂NPs/CPE was tested for repeatability, reproducibility, and stability, and the results support the sensor's good characteristics. The selectivity of the proposed method was studied, and the results showed that there was no disruption in the detection of zileuton, and that the peak current changed by less than 5%. Finally, BiOCl/CuS@SnO₂NPs/CPE was successfully used to determine zileuton in pharmaceutical formulations and human serum samples, with recovery rates ranging from 98.3% percent to 103.6% percent and an RSD of less than 5%.

Keywords: Nanocomposite, Zileuton, Carbon Paste Electrode, modified.

[a]. Department of Chemistry, College of Science and Arts - Sharourah, Najran University, Sharourah, Saudi Arabia.

[b]. Department of Chemistry, College of Science, Ibb University, Ibb, Yemen.

Email: dralhemiary@gmail.com

DOI: 10.31838/ecb/2022.11.09.011

INTRODUCTION

Zileuton (N-(1-(benzo[b]thien-2-yl) ethyl)-N-hydroxyurea) (Figure 1) exhibits almost equivalent therapeutic efficacy (Ganorkar and Shirkhedkar 2017). Zileuton is a 5-lipoxygenase inhibitor that is active when taken orally and lowers the generation of leukotrienes, making it a popular asthma maintenance medication (Bailie et al. 1995)(Lim et al. 2019). Zileuton is a 5-lipoxygenase inhibitor that is active when taken orally and lowers the generation of leukotrienes, making it a popular asthma maintenance medication (Sorkness 1997) Leukotrienes with sulfido-peptides (LTC₄, LTD₄, LTE₄) (Gounaris et al. 2015)(Morina et al. 2016). Several bodily fluids can be used to assess leukotriene A₄ (LTA₄), the first unstable byproduct of arachidonic acid metabolism, and LTB₄, a chemoattractant for neutrophils and eosinophils (You et al. 2020). In asthmatic patients, zileuton pretreatment reduced bronchoconstriction caused by a cold air challenge(Drazen, Israel, and O'byrne 1999)(Magazine et al. 2016). A review of the literature revealed that UV and VIS spectrophotometry(Rao et al. 2015), HPLC(Pian et al. 2013), LC/MSMS(PRAKASH, ADIKI, and KALAKUNTALA 2014), HPTLC and

UVAUC(Ganorkar and Shirkhedkar 2017), RP-HPLC-PDA(Ganorkar, Dhupal, and Shirkhedkar 2017) polarography(Sreedhar et al. 2010) Glass carbon electrode(Nabil A. Alhemiary. 2017), and polymer carbon paste electrode(Baezzat, Bagheri, and Abdollahi 2019) for effective analytical findings of zileuton in pharmaceutical dosage forms and biological fluids, are very significant, diversified, and unusual reports (Nabil A. Alhemiary. 2017).

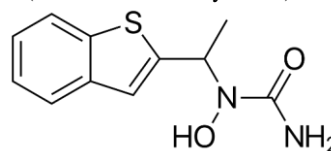


Figure 1: Zileuton chemical structure.

There are only a few papers in the realm of electrochemistry that mention zileuton measuring. Glassy carbon electrodes have been used to determine zileuton in two published studies (Baezzat, Bagheri, and Abdollahi 2019)(Elqudaby et al. 2013)(Nabil A. Alhemiary. 2017). In recent experiments polymer Carbon paste electrode based sensor for measuring zileuton has been used for zileuton oxidation (Baezzat, Banavand, and Fasihi 2019)(Baezzat, Bagheri, and Abdollahi 2019). As a result, CPE is generally utilized for low-detection-limit electrochemical measurements of a range of compound species. Bismuth oxy-chloride (BiOCl) has long been used as a selective oxidation catalyst, photo-catalyst, and photoluminescence due to its significant electrical, optical, and catalytic properties (Sun et al. 2019)(Qian et al. 2020). A halogen atom is sandwiched between two layers of [Bi₂O₂] in

this layered or laminated semiconductor (Bao and Yuan 2020). CuS has electrical conductivity similar to metal and effective chemical sensing properties (Maheshwaran et al. 2021). It is widely used in a variety of processes, including the production of high-capacity cathodes for lithium batteries (Chung and Sohn 2002), thin films (Yuan et al. 2008), solar cells (Congiu et al. 2016), nanometer scale switches (Sakamoto et al. 2003), catalysis, superionic conductor, sensors, optical filters (Shuai et al. 2018), electronic, optoelectronic and solar radiation absorbers applications, as well as environmental processes like photocatalytic applications for dye degradation (Shuai et al. 2018), water purification, waste water treatment (Maji et al. 2011), water treatment at room temperature (Andronic, Isac, and Duta 2011), and room temperature ammonia sensors (Aljohani and Al-Aoh 2021) (Galdikas et al. 2000). Recently, nanocrystalline copper sulfide has been used to create superconductors, hydrogen sulfide sensors, ion selective electrodes, and photoelectric transformers (Han et al. 2011) (Saranya and Nirmala Grace 2012). SnO₂NPs are useful in a variety of applications, including lithium-ion batteries, solar cells, optoelectronics, and catalytic processes including the breakdown of methyl violet and methylene blue (Bhattacharjee, Ahmaruzzaman, and Sinha 2015) (Kim, Choi, and Choi 2016) (Chandra et al. 2019) (Cui et al. 2018). Due to their outstanding chemical stability and optical and electrical qualities (Gao et al. 2014). As a result, using the sulfur-copper@tin oxide nanocomposite for sensitive sensor manufacturing could be a promising option (Asfaram et al. 2018) (Al-Hamdi and Sillanpää 2020). Furthermore, the hybridization of BiOCl, CuS, and SnO₂ could be used to change electrodes by increasing the electrode surface and electrical conductivity. These NPs also have the potential to speed up the transport of electrons from a wider variety of electroactive materials to the electrode surface. The current paper explains how to make an efficient nanocomposite out of BiOCl/CuS@SnO₂NPs with large surface areas and catalytic properties for this purpose. To identify zileuton in pharmaceutical formulations and serum samples. We developed a novel chemically modified CPE based on the BiOCl/CuS@SnO₂NPs/CPE nanocomposite (Scheme 1).

EXPERIMENTAL

Reagents and Chemicals:

Sigma-Aldrich provided the zileuton standard powder (purity 99.8%). Each aqueous solution was prepared using distilled water. Graphite powder, Cu(NO₃)₂·3H₂O, NH₄CH₃COO, CH₃CSNH₂, Bi(NO₃)₃·5H₂O, SnCl₄, NaOH, SnCl₂, HCl, H₂SO₄, H₃PO₄, H₂O₂, FeSO₄, and the solvents were among the chemicals and reagents that were acquired from Merck (Germany) and Aldrich. We utilized (0.1M) phosphate buffer solution as the electrolyte. The Sharourah Hospital provided the human blood serum sample (Sharourah- Saudi Ariba).

The weighed amount of 1.0 × 10⁻⁴ M zileuton stock solution was freshly made by combining it with de-ionized water, then stored in a PVC container in the refrigerator. between pH 3.0-9.0, 0.1 M phosphate buffer. Standard solutions were created by serially diluting the stock solution with a supporting electrolyte that was carefully chosen. It was possible to produce the calibration curves for DPV analysis by plotting the peak current versus zileuton concentration.

Apparatus:

The voltametric experiments used a computerized Metrohm voltametric analyzer model 797 VA with Software Version 1.0. Three electrodes were used in the setup: a Pt wire counter electrode, working electrodes made of CPE and modified CPE (used separately), and an Ag/AgCl reference electrode (3 mol/L KCl). Using a digital pH/mV meter (JEANWAY 3510) and a glass combination electrode, the buffer solution was made. Using an Eppendorf-multipipette and micropipette, the current experiment was carried out.

Preparing the BiOCl/CuS:

For the synthesis of BiOCl/CuS, put 0.2175 g Bi(NO₃)₃·5H₂O and 0.336 g KCl in a mixing bowl. After that, add 30 ml ethylene glycol and 15 ml ethanol, and stir for 10 minutes. Following that, the aforementioned solution was mixed with 0.1098 g of Cu(NO₃)₂·3H₂O and shaken for 20 minutes. The mixture was then given 3 mL of mercaptoacetic acid, and it was stirred for 10 minutes at room temperature. CuS/BiOCl was hydrothermally synthesized for six hours at 160 °C, the mixture was then placed in a stainless-steel autoclave lined with Teflon. Next, room temperature was gradually reached using the autoclave. Following filtration, the precipitate underwent ethanol and distilled water washings. Finally, BiOCl/CuS was produced by drying the nanocomposite at 60 °C under vacuum for 24 hours (Mohammadzadeh Jahani, Akbari Javar, and Mahmoudi-Moghaddam 2020).

Preparation of SnO₂NPs

The SnO₂NPs were synthesized based on the literature (Asfaram et al. 2018) (Naghian and Najafi 2018) First, 8.0 mL each of a 1.0 M NH₄CH₃CO₂ solution and a 0.5 M SnCl₂ aqueous solution were combined while stirring. SnCl₄ 8% (V/V) aqueous solution and 10.0 mL of 0.4 M CH₃CSNH₂ solution were then added to the initial mixed solution and stirred for 30 minutes. The created mixed solution was diluted with de-ionized water to a final volume of 150 mL. The produced reaction solution was then heated to 80 °C in an autoclave for 24 hours. Following a centrifugation of the mixture at 8000 rpm, de-ionized water was used to repeatedly wash the separated nanoparticles. The nanoparticles were then dried on 0.45 m Porosity filter paper for 24 hours at 50 °C.

Preparation of BiOCl/CuS@SnO₂NPs:

The SnO₂NPs were obtained and mixed with the BiOCl/CuS solution (1 mg/ml, 50 ml) after being cleaned with distilled water. After that, the mixture was placed in a stainless steel autoclave with a 100 mL Teflon liner and heated to 120 °C for 12 hours. The BiOCl/CuS@SnO₂NPs were dried in the autoclave for 24 hours at 60 °C after cooling it.

Fabrication of the BiOCl/CuS@SnO₂NPs/CPE

0.15 g of synthetic BiOCl/CuS@SnO₂NPs were combined with 0.01 g of graphite to make a mortar. A suitable paste was then created by adding 0.1 mL of paraffin oil and stirring. A Teflon tube with a 2 mm inner diameter was fitted with copper wire after the paste had been tightly packed inside it to create an electrical connection. On one piece of tiny aluminum foil, the wide head of the resultant electrode was smoothed. A CPE was made in the same way as the BiOCl/CuS@SnO₂NPs, but with graphite powder instead of BiOCl/CuS@SnO₂NPs in the manufacturing technique.

Electrochemical analysis's process.:

The tests were conducted in a phosphate buffer of 0.1 M. Differential pulse voltammograms with an amplitude of 0.08 V, a pulse period of 0.5 seconds, an equilibration time of 4 seconds, a pulse width of 0.05 seconds, and were created by

adjusting the parameters. The impedance research was carried out at open circuit potential, with oscillation potential ranging from 200,000 Hz to 0.1 Hz, and oscillation potential of 0.005 V (Naghian and Najafi 2018).

Real-life sample preparation

The tablet formulation was offered on the Saudi Arabian market, and each tablet contained 600 mg of zileuton. In a mortar, ten zileuton tablets were crushed into a fine powder. This powder was appropriately weighed, and 100 mL of water was added before it was ultrasonically dissolved. The diluted solution was then divided into separate portions and transferred to a 25 mL volumetric flask where it was diluted with a 0.1 M phosphate buffer solution (pH=8) to the required concentration. (Nabil A. Alhemiary. 2017). In addition, we used our new technique to analyze zileuton content using the standard addition method. Furthermore, we obtained human blood Serum samples from five healthy volunteers from Sharourah hospital in Saudi Arabia; therefore, the samples were centrifuged (5000 rpm) for 30 minutes at ambient temperature ($25 \pm 0.1^\circ\text{C}$) and separated. After that, they were diluted with a pH 8.0 phosphate buffer solution (Mohammadzadeh Jahani, Akbari Javar, and Mahmoudi-Moghaddam 2020).

RESULTS AND DISCUSSION

Characterization of nanocomposite:

Fig 2 displays the XRD images of SnO_2 , BiOCl/CuS , and $\text{BiOCl/CuS}@ \text{SnO}_2$ NPs. The prominent peaks at 2θ are 110° , 211° , and 101° (Figure. 2a), showing that SnO_2 is rutile in structure (JCPDS card: 41-1445). Figure 3b displays the BiOCl/CuS nanocomposite XRD pattern. According to Wang's recent study on the fabrication of BiOCl/CuS nanocomposite, With the standard cards of BiOCl (JCPDS 06-0249) and CuS (JCPDS No. 06-0464), all the curve's principal diffraction peaks are compatible. (Wang et al. 2015). The XRD pattern of $\text{BiOCl/CuS}@ \text{SnO}_2$ NPs (Figure 2c) shows the unique diffraction peaks of three SnO_2 , BiOCl , and CuS crystalline phases, and the sharp and intense peaks indicate that the

synthesized nanocomposite is well crystallized. Because BiOCl/CuS was partially substituted with the crystalline phase of SnO_2 NPs during the formation of the nanocomposite, as shown in Figure.2c, the presence of BiOCl/CuS reduced the intensity of the principal characteristic peaks of SnO_2 NPs (110 and 200). It is worth noting that Debye-Scherrer Eq (1) (MacDonald et al. 2016) is noteworthy.

$$D = \frac{0.9\lambda}{\beta \cos\theta} \quad (1)$$

It was utilized to compute the crystallite dimension (D) from the figure's most important peak. Where is the whole width at half-maximum, is the diffraction angle, and is the X-ray wavelength (1.54056 for a Cu lamp). SnO_2 NPs crystallite dimensions of 17.7 nm and BiOCl/CuS crystallite dimensions of 48.9 nm were obtained using Eq. 1.

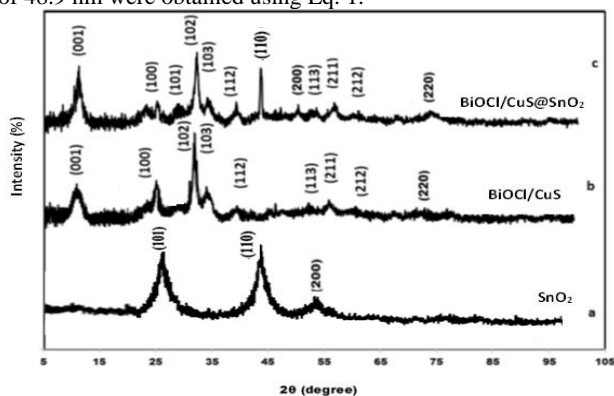


Figure 2: XRDs of SnO_2 , CuS/BiOCl/CuS , and the $\text{BiOCl/CuS}@ \text{SnO}_2$ nanocomposite, respectively, in (a), (b), and (c).

The $\text{BiOCl/CuS}@ \text{SnO}_2$ NPs' surface morphology was investigated using the SEM technique. Figure 3A's SEM picture of the $\text{BiOCl/CuS}@ \text{SnO}_2$ NPs exhibits a uniform distribution of spherical nanoparticles with a diameter of roughly 10 to 30 nm.

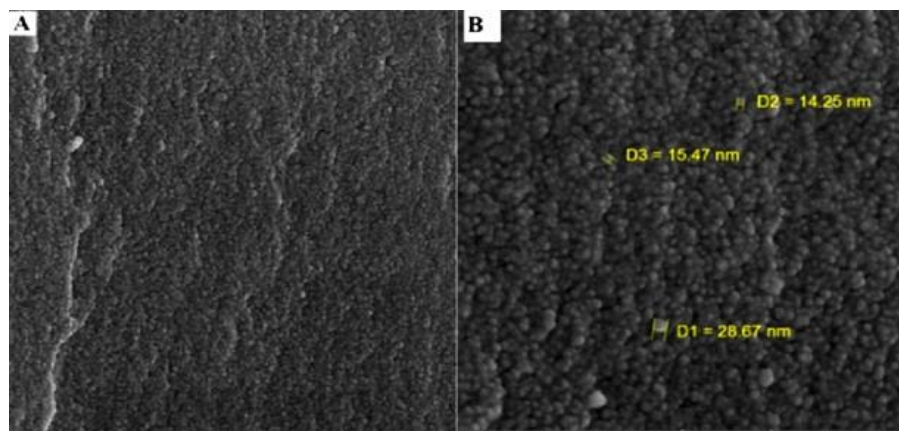


Figure 3: $\text{BiOCl/CuS}@ \text{SnO}_2$ NPs SEM images (A) 100 Kx and (B) 200 Kx

Electrochemical characterization:

The performance of the CPE and $\text{BiOCl/CuS}@ \text{SnO}_2$ NPs/CPE was measured using a cyclic voltammetry approach. For this, electrochemical measurements of 1 mM $\text{Fe}(\text{CN})_6^{3/4-}$ in 0.1 M Na_2HPO_4 at potentials between -0.35 and 0.75 V were used.

The $\text{Fe}(\text{CN})_6^{3/4-}$ redox peaks are quite feeble at the exposed CPE surface. Peak differences between oxidation and reduction peaks for $\text{Fe}(\text{CN})_6^{3/4-}$ solution were larger when the CPE was modified with $\text{BiOCl/CuS}@ \text{SnO}_2$ NPs, at 0.19 V, than the CPE, indicating that the modified CPE had a higher electron rate than

the CPE. The electrochemical impedance measurements in a solution of $\text{Fe}(\text{CN})_6^{3-/4-}$ confirmed these findings, showing that CPE has a transfer resistance of 0.64 k, while $\text{BiOCl}/\text{CuS}@/\text{SnO}_2\text{NP}/\text{CPE}$ has a transfer resistance of 0.24 k, indicating that the latter has better charge transfer kinetics and facilitates electron transfer (Ghanbari et al. 2019)(Khoshroo et al. 2019)(Tajik et al. 2020). Voltammograms produced from several electrodes in $\text{Fe}(\text{CN})_6^{3-/4-}$ solution are shown in Figure 4A. Figure 4B shows the electrochemical impedance results. The cyclic voltammograms of zileuton on bare CPE and $\text{BiOCl}/\text{CuS}@/\text{SnO}_2\text{NPs}/\text{CPE}$ in 0.1 M phosphate buffer solution (pH = 8) accumulation duration of 90s, perturbation amplitude: 5 mV, with Scan rate 50 mV s⁻¹, EIS condition: frequency range: 200 KHz - 0.1 Hz, are shown in Figure 4C. The scans (a) and (b) show zileuton (1×10^{-4} M) cyclic voltammograms on the bare electrode and scan (b) $\text{BiOCl}/\text{CuS}@/\text{SnO}_2\text{NPs}/\text{CPE}$ cyclic voltammograms in the same solution. A single irreversible oxidation peak is visible over the voltage window in the cyclic voltammograms of both electrodes (0.5 to 1.3 V).

When compared to Ag/AgCl , the $\text{BiOCl}/\text{CuS}@/\text{SnO}_2\text{NPs}/\text{CPE}$ modified electrode displays a considerable oxidation current starting at 640 mV. The zileuton current was started at around 0.8 V, and this result reveals little redox activity at the bare CPE over the same potential range. $\text{BiOCl}/\text{CuS}@/\text{SnO}_2\text{NPs}/\text{CPE}$ exhibits significant catalytic activity for the electrooxidation of zileuton as evidenced by the strong negative shift in the onset potential and the significant rise in zileuton peak current. 1×10^{-4} M zileuton is present in 0.1 M phosphate buffer solution with pH=8. $\text{BiOCl}/\text{CuS}@/\text{SnO}_2\text{NPs}'$ cyclic voltammograms were studied, and the results are shown in Figure 5A. The impact of a scan rate between 10 and 500 mVs^{-1} was considered. Figure 5B also displays plots of the electro-oxidation of zileuton peak currents as a function of the logarithm. Anodic current logarithms and scan rate exhibit linear correlations. This demonstrates that a mixed adsorption-diffusion on the $\text{BiOCl}/\text{CuS}@/\text{SnO}_2\text{NPs}/\text{CPE}$ affects the overall process kinetics.

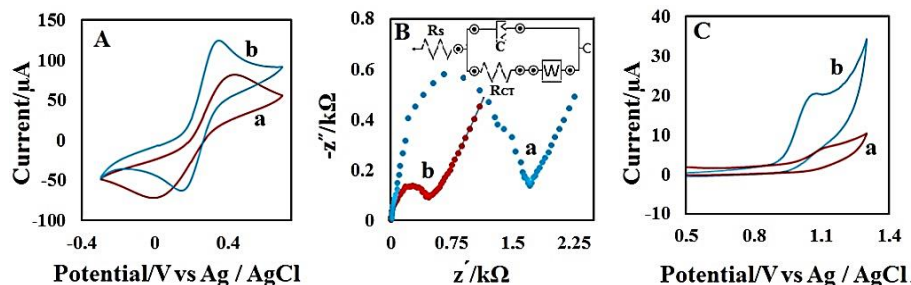


Figure 4: (A) Cyclic voltammetry of the CPE surface (a) $\text{BiOCl}/\text{CuS}@/\text{SnO}_2\text{NPs}/\text{CPE}$ (b) with a scan rate of 50 mVs^{-1} in the probe redox. (B) It was noted in the probe redox, as shown in (a) by the Nyquist plot of the CPE and (b) by the $\text{BiOCl}/\text{CuS}@/\text{SnO}_2\text{NPs}/\text{CPE}$. (C) $\text{BiOCl}/\text{CuS}@/\text{SnO}_2\text{NPs}/\text{CPE}$ cyclic voltammograms (a) and (b) in the presence of 1×10^{-4} M zileuton in the phosphate buffer solution at pH=8 at a scan rate of 50 mVs^{-1} and accumulation duration of 90 s.

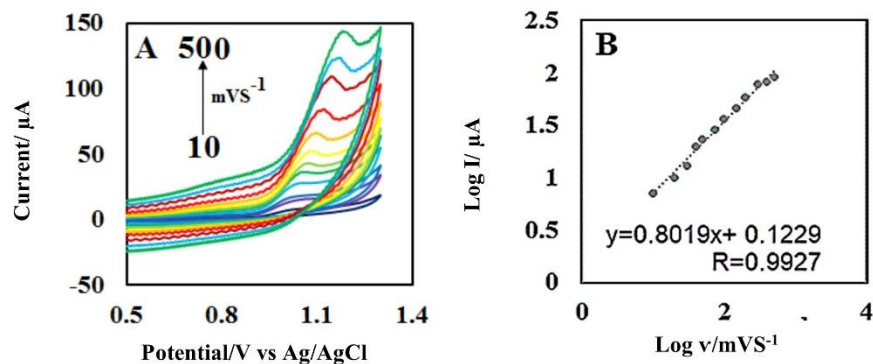


Figure 5. (A) The influence of scan rate on the cyclic voltammograms response to 1×10^{-4} M zileuton (pH=8) with accumulation period 90 s at $\text{BiOCl}/\text{CuS}@/\text{SnO}_2\text{NPs}/\text{CPE}$ electrode with a range of scan rates (10 to 500 mVs^{-1}). (B) The relationship between logarithm scan rate and logarithm peak currents..

The optimization of pH:

It is widely known that the pH of the aqueous solution affects the electrochemical activity of zileuton. To observe reasonable results for zileuton electro-oxidation, the pH of the solution must be optimized. So, using a 0.1 M phosphate buffer solution with a pH range of 3.0 to 9.0, DPV voltammograms have been taken to study the electrochemical behavior of zileuton. The

neutral pH is more conducive to zileuton electro-oxidation at the $\text{BiOCl}/\text{CuS}@/\text{SnO}_2\text{NPs}/\text{CPE}$ surface than the basic or acidic media, as illustrated in Figure 6B, where the highest current was obtained at pH 8. As a result, pH 8.0 was selected as the best pH for electro-oxidation of zileuton at the $\text{BiOCl}/\text{CuS}@/\text{SnO}_2\text{NPs}/\text{CPE}$ surface.

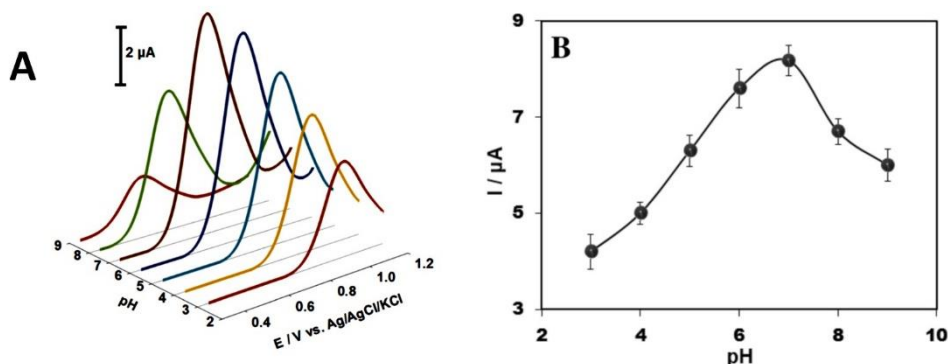


Figure 6: (A): Voltammograms produced by differential pulse voltammetry of 300.0 μM zileuton in phosphate buffer solution with a pH range of 3 to 9. (B): The I_p of zileuton as a function of pH ($n = 3$)

The Analytical Procedure's Validation

The DPV curves produced by $\text{BiOCl/CuS@SnO}_2\text{NPs/CPE}$ using phosphate buffer are shown in Figure 7(A) in the presence of varied zileuton concentrations (0.1 M, pH 8). It was discovered that increasing zileuton concentrations enhanced the I_p of zileuton. In addition, the ratio of peak current to zileuton concentration was linear (Figure. 7B). In addition, regression equation $I_p = 0.4145X - 1.1420$; $R^2 = 0.9938$ was used to fit the calibration plot. Moreover, $\text{BiOCl/CuS@SnO}_2\text{NPs/CPE}$

demonstrated a linear range from 4 to 75 μM , with a LOD of 0.07 μM determined for zileuton.

Comparing the sensor to other zileuton sensors previously disclosed, Table 1 demonstrates that it has a similar or even better sensitivity (as determined by the slope of the calibration curve), a lower LOD and a greater linear dynamic range. The remarkable performance of the sensor is due to the increased effective surface area of $\text{BiOCl/CuS@SnO}_2\text{NPs/CPE}$ (Naghian and Najafi 2018)(He et al. 2014)(Dehbashi et al. 2013).

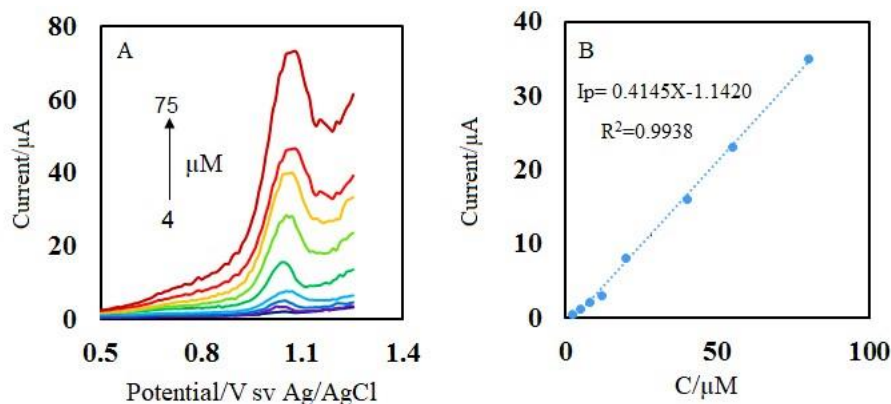


Figure 7 (A): The recorded DPV for various concentrations of zileuton from 4-75 μM on $\text{BiOCl/CuS@SnO}_2\text{NPs/CPE}$ in phosphate buffer (pH=8), and (B) $\text{BiOCl/CuS@SnO}_2\text{NPs/CPE}$ in phosphate buffer with a relative calibration curve and a 90 s accumulation time.

Table 1 shows the analytical features for determining zileuton using a variety of methods.

Type Electrode	Method	pH	LOD (μM)	Liner range (μM)	Reference
Glassy carbon	DPV	8	0.13	2-120	(Nabil A. Alhemiary. 2017)
Glassy carbon	SWV	8	0.03	1-180	(Nabil A. Alhemiary. 2017)
MIP-modified carbon paste	DPV	7	0.8	4-105	(Baezzat, Bagheri, and Abdollahi 2019)
$\text{BiOCl/CuS@SnO}_2\text{NPs/CPE}$	DPV	8	0.07	4-75	This study

The sensor functions are defined by their repeatability, reproducibility, and stability (Cui et al. 2018). Furthermore, the

relative standard deviation (RSD) for measuring 30 μM zileuton with DPV at five different electrodes obtained in the same way

was 2.95 %. This suggests that $\text{BiOCl/CuS}@ \text{SnO}_2 \text{NPs}/\text{CPE}$ is very reproducible. In addition, five repeated measurements of zileuton detection using DPV at a modified electrode with an RSD of 2.18% were performed to verify repeatability. We also tested the sensor's stability by keeping it at room temperature for four weeks and measuring the zileuton twice a week. Our sensor maintained 94% of initial response after the delay, indicating that $\text{BiOCl/CuS}@ \text{SnO}_2 \text{NPs}/\text{CPE}$ is reasonably stable.

Interfering species' effect

We investigated the selectivity of our sensor in ideal conditions while detecting zileuton (30 μM), and investigated interference from a range of foreign elements, including several organic and inorganic substances. Furthermore, the tolerance threshold was established at the highest amount of foreign pollutants that resulted in a relative error of $\sim \pm 5\%$ when the analyte was detected. There was no interference in detecting zileuton with

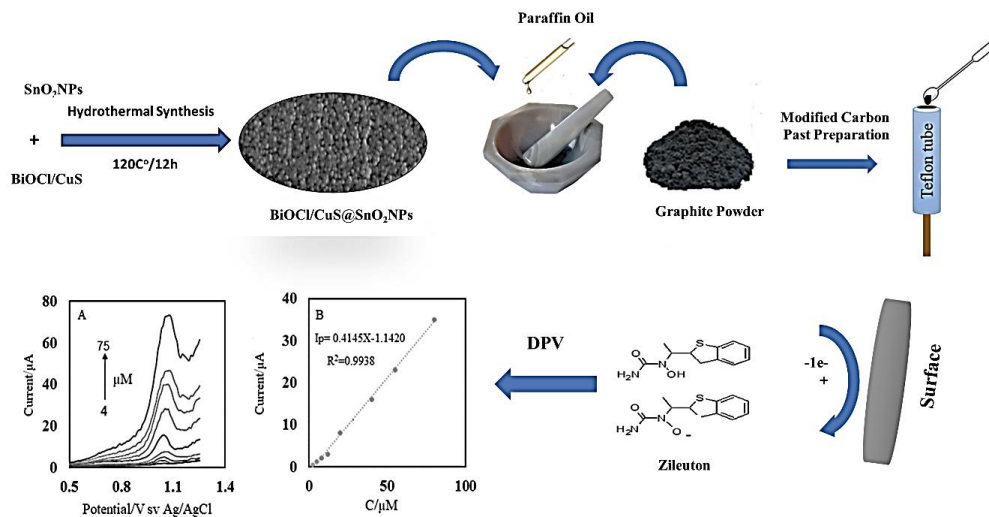
1mM concentrations of NH_4^+ , K^+ , Na^+ , Mg^{2+} , Ca^{2+} , NO_3^- , CO_3^{2-} , Cl^- , SO_4^{2-} , acetaminophen, dopamine, fructose, sucrose, glucose, fructose, oxalate, citric acid, ascorbic acid, and cysteine. $\text{BiOCl/CuS}@ \text{SnO}_2 \text{NPs}/\text{CPE}$ has thus been shown to have a decent selectivity for zileuton detection.

Real-life sample analysis

To assess the method's potential, zileuton concentrations in pharmaceutical formulations and protein-free spiking human serum samples were measured using differential pulse voltammetry response at the surface of a $\text{BiOCl/CuS}@ \text{SnO}_2 \text{NPs}/\text{CPE}$ electrode. Additionally, a typical addition method was used to find zileuton in real specimens. The analyses' findings are presented in Table 2. The percentage of recovery in the triplicate studies ranged from 98.3 % to 103.6 %, with RSDs of less than 5%. As a result, zileuton can be successfully assayed in these samples using the $\text{BiOCl/CuS}@ \text{SnO}_2 \text{NPs}/\text{CPE}$ electrode.

Table 2. Using $\text{BiOCl/CuS}@ \text{SnO}_2 \text{NPs}/\text{CPE}$, zileuton was determined in a real-life sample analysis (n=3).

Sample	Added (μM)	Found (μM)	Recovery %	RSD %
Zileuton tablet	0.0	5	-	2.6
	4	9.10	101.1	3.1
	10	14.94	99.6	2.8
	15	20.38	98.13	2.5
Seram	0	N.D	-	-
	5	4.96	99.2	1.8
	10	10.29	102.9	3.0
	15	15.54	103.6	2.4



Scheme 1: Modification of a sensor for the detection of zileuton

CONCLUSION

The $\text{BiOCl/CuS}@ \text{SnO}_2 \text{NPs}/\text{CPE}$ system provides electroactive sites for the accumulation of zileuton. The differential pulse voltammetry method was utilized to determine zileuton with a low detection limit. This electrode is easy to make and has a high selectivity for determining zileuton. When compared to an unmodified electrode, the overpotential for fentanyl oxidation at the surface of this modified electrode is lower. The modified electrode also increased the electro-oxidation peak current of

zileuton in comparison to the unmodified CPE. Serum samples and pharmaceutical formulations both responded favorably to zileuton measurement using the modified electrode.

ACKNOWLEDGMENTS

This study was funded by Deanship of Scientific Research of Najran University, Kingdom of Saudi Arabia, No. NU/ESCI/20/101.

Conflict of interest: The author declare that they have no known competing financial interests or personal relationships

that could have appeared to influence the work reported in this paper.

REFERENCES

- i. Al-Hamdi, Abdullah, and Mika Sillanpää. 2020. *Photocatalytic Activities of Antimony, Iodide, and Rare Earth Metals on SnO₂ for the Photodegradation of Phenol under UV, Solar, and Visible Light Irradiations*. *Advanced Water Treatment: Advanced Oxidation Processes*. <https://doi.org/10.1016/B978-0-12-819225-2.00004-1>.
- ii. Aljohani, Meshari M.H., and Hatem A. Al-Aoh. 2021. "Adsorptive Removal of Permanganate Anions from Synthetic Wastewater Using Copper Sulfide Nanoparticles." *Materials Research Express* 8 (3). <https://doi.org/10.1088/2053-1591/abef40>.
- iii. Andronic, Luminita, Luminita Isac, and Anca Duta. 2011. "Photochemical Synthesis of Copper Sulphide/Titanium Oxide Photocatalyst." *Journal of Photochemistry and Photobiology A: Chemistry* 221 (1): 30–37.
- iv. Asfaram, Arash, Mehrorang Ghaedi, Hamedreza Javadian, and Alireza Goudarzi. 2018. "Cu- and S-@SnO₂ Nanoparticles Loaded on Activated Carbon for Efficient Ultrasound Assisted Dispersive MSPE-Spectrophotometric Detection of Quercetin in Nasturtium Officinale Extract and Fruit Juice Samples: CCD-RSM Design." *Ultrasonics Sonochemistry* 47 (April): 1–9. <https://doi.org/10.1016/j.ultsonch.2018.04.008>.
- v. Baezzat, Mohammad Reza, Maryam Bagheri, and Elaheh Abdollahi. 2019. "Molecularly Imprinted Polymer Based Sensor for Measuring of Zileuton: Evaluation as a Modifier for Carbon Paste Electrode in Electrochemically Recognition." *Materials Today Communications* 19: 23–31. <https://doi.org/10.1016/j.mtcomm.2018.12.013>.
- vi. Baezzat, Mohammad Reza, Fatemeh Banavand, and Farshid Fasihi. 2019. "Highly Sensitive Determination of Zileuton Using TiO₂ Nanoparticles and the Ionic Liquid 1-Hexylpyridinium Hexafluorophosphate Nanocomposite Sensor." *Ionics: International Journal of Ionics The Science and Technology of Ionic Motion* 25 (4): 1835–44. <https://doi.org/10.1007/s11581-018-2699-8>.
- vii. Bailie, Marc B, Lawrence J Dahm, Marc Peters-Golden, Richard R Harris, George W Carter, and Robert A Roth. 1995. "Leukotrienes and α -Naphthylisothiocyanate-Induced Liver Injury." *Toxicology* 100 (1–3): 139–49.
- viii. Bao, Liang, and Yong-Jun Yuan. 2020. "Highly Dispersed BiOCl Decahedra with a Highly Exposed (001) Facet and Exceptional Photocatalytic Performance." *Dalton Transactions* 49 (33): 11536–42.
- ix. Bhattacharjee, Archita, M Ahmaruzzaman, and Tanur Sinha. 2015. "A Novel Approach for the Synthesis of SnO₂ Nanoparticles and Its Application as a Catalyst in the Reduction and Photodegradation of Organic Compounds." *Spectrochimica Acta Part A: Molecular and Biomolecular Spectroscopy* 136: 751–60.
- x. Chandra, Ramesh, Vedita Singh, Shailly Tomar, and Mala Nath. 2019. "Multi-Core-Shell Composite SnO₂NPs@ ZIF-8: Potential Antiviral Agent and Effective Photocatalyst for Waste-Water Treatment." *Environmental Science and Pollution Research* 26 (23): 23346–58.
- xi. Chung, J.-S., and H.-J. Sohn. 2002. "Electrochemical Behaviors of CuS as a Cathode Material for Lithium Secondary Batteries." *Journal of Power Sources* 108 (1): 226–31. [https://doi.org/https://doi.org/10.1016/S0378-7753\(02\)00024-1](https://doi.org/https://doi.org/10.1016/S0378-7753(02)00024-1).
- xii. Congiu, M, O Nunes-Neto, M L De Marco, D Dini, and C F O Graeff. 2016. "Cu₂-xS Films as Counter-Electrodes for Dye Solar Cells with Ferrocene-Based Liquid Electrolytes." *Thin Solid Films* 612: 22–28. <https://doi.org/https://doi.org/10.1016/j.tsf.2016.05.033>.
- xiii. Cui, Xiaoqing, Xian Fang, Hong Zhao, Zengxi Li, and Hongxuan Ren. 2018. "Fabrication of Thiazole Derivatives Functionalized Graphene Decorated with Fluorine, Chlorine and Iodine@ SnO₂ Nanoparticles for Highly Sensitive Detection of Heavy Metal Ions." *Colloids and Surfaces A: Physicochemical and Engineering Aspects* 546: 153–62.
- xiv. Dehbashi, Mohsen, Mousa Aliahmad, Mohammad Reza Mohammad Shafiee, and Majid Ghashang. 2013. "Nickel-Doped SnO₂ Nanoparticles: Preparation and Evaluation of Their Catalytic Activity in the Synthesis of 1-Amido Alkyl-2-Naphtholes." *Synthesis and Reactivity in Inorganic, Metal-Organic, and Nano-Metal Chemistry* 43 (9): 1301–6.
- xv. Drazen, Jeffery M, Elliot Israel, and P M O'byrne. 1999. "Drug Therapy: Treatment of Asthma with Drugs Modifying the Leukotriene Pathway." *New England Journal of Medicine* 340: 197–206.
- xvi. Elqudaby, H M, Gehad G Mohamed, F A Ali, and Sh M Eid. 2013. "Validated Voltammetric Method for the Determination of Some Antiprotozoa Drugs Based on the Reduction at an Activated Glassy Carbon Electrode." *Arabian Journal of Chemistry* 6 (3): 327–33.
- xvii. Galdikas, A, A Mironas, V Strazdien, A Setkus, I Ancutien, and V Janickis. 2000. "Room-Temperature-Functioning Ammonia Sensor Based on Solid-State CuxS Films." *Sensors and Actuators B: Chemical* 67 (1–2): 76–83.
- xviii. Ganorkar, Saurabh B., Dinesh M. Dhumal, and Atul A. Shirkhedkar. 2017. "Development and Validation of Simple RP-HPLC-PDA Analytical Protocol for Zileuton Assisted with Design of Experiments for Robustness Determination." *Arabian Journal of Chemistry* 10 (2): 273–82. <https://doi.org/10.1016/j.arabjc.2014.03.009>.
- xix. Ganorkar, Saurabh B, and Atul A Shirkhedkar. 2017. "Novel HPTLC and UV-AUC Analyses: For Simple, Economical, and Rapid Determination of Zileuton Racemate." *Arabian Journal of Chemistry* 10 (3): 360–67. <http://10.0.3.248/j.arabjc.2013.05.013>.
- xx. Gao, Yilong, Jianxiang Wu, Wei Zhang, Yueyue Tan,

- Jiachang Zhao, and Bohejin Tang. 2014. "The Electrochemical Performance of SnO₂ Quantum Dots@ Zeolitic Imidazolate Frameworks-8 (ZIF-8) Composite Material for Supercapacitors." *Materials Letters* 128: 208–11.
- xxi. Ghanbari, Mohammad Hossein, Alireza Khoshroo, Hossein Sobati, Mohammad Reza Ganjali, Mehdi Rahimi-Nasrabadi, and Farhad Ahmadi. 2019. "An Electrochemical Sensor Based on Poly (L-Cysteine)@ AuNPs@ Reduced Graphene Oxide Nanocomposite for Determination of Levofloxacin." *Microchemical Journal* 147: 198–206.
- xxii. Gounaris, Elias, Michael J Heiferman, Jeffrey R Heiferman, Manisha Shrivastav, Dominic Vitello, Nichole R Blatner, Lawrence M Knab, Joseph D Phillips, Eric C Cheon, and Paul J Grippo. 2015. "Zileuton, 5-Lipoxygenase Inhibitor, Acts as a Chemopreventive Agent in Intestinal Polyposis, by Modulating Polyp and Systemic Inflammation." *PLoS One* 10 (3): e0121402.
- xxiii. Han, Yan, Yaping Wang, Wenhong Gao, Yijing Wang, Lifang Jiao, Huatang Yuan, and Shuangxi Liu. 2011. "Synthesis of Novel CuS with Hierarchical Structures and Its Application in Lithium-Ion Batteries." *Powder Technology* 212 (1): 64–68.
- xxiv. He, Chenglong, Yong Xiao, Hanwu Dong, Yingliang Liu, Mingtao Zheng, Ke Xiao, Xiangrong Liu, Haoran Zhang, and Bingfu Lei. 2014. "Mosaic-Structured SnO₂@ C Porous Microspheres for High-Performance Supercapacitor Electrode Materials." *Electrochimica Acta* 142: 157–66.
- xxv. Khoshroo, Alireza, Laleh Hosseinzadeh, Ali Sobhani-Nasab, Mehdi Rahimi-Nasrabadi, and Farhad Ahmadi. 2019. "Silver Nanofibers/Ionic Liquid Nanocomposite Based Electrochemical Sensor for Detection of Clonazepam via Electrochemically Amplified Detection." *Microchemical Journal* 145: 1185–90.
- xxvi. Kim, Sung Phil, Myong Yong Choi, and Hyun Chul Choi. 2016. "Photocatalytic Activity of SnO₂ Nanoparticles in Methylene Blue Degradation." *Materials Research Bulletin* 74: 85–89.
- xxvii. Lim, Hyun-Joung, Jinbong Park, Jae-Young Um, Sang-Seob Lee, and Hyun-Jeong Kwak. 2019. "Zileuton, a 5-Lipoxygenase Inhibitor, Exerts Anti-Angiogenic Effect by Inducing Apoptosis of HUVEC via BK Channel Activation." *Cells* 8 (10): 1182.
- xxviii. MacDonald, M J, J Vorberger, E J Gamboa, R P Drake, S H Glenzer, and L B Fletcher. 2016. "Calculation of Debye-Scherrer Diffraction Patterns from Highly Stressed Polycrystalline Materials." *Journal of Applied Physics* 119 (21): 215902.
- xxix. Magazine, Rahul, Hameed Shahul, Bharti Chogtu, and Asha Kamath. 2016. "Comparison of Oral Montelukast with Oral Zileuton in Acute Asthma: A Randomized, Double-Blind, Placebo-Controlled Study." *Lung India* 33 (3): 281–86. <https://doi.org/10.4103/0970-2113.180805>.
- xxx. Maheshwaran, Selvarasu, Ramachandran Balaji, Shen-Ming Chen, Ray Biswadeep, Vengudusamy Renganathan, Chandrasekar Narendhar, and C R Kao. 2021. "Copper Sulfide Nano-Globules Reinforced Electrodes for High-Performance Electrochemical Determination of Toxic Pollutant Hydroquinone." *New Journal of Chemistry* 45 (6): 3215–23.
- xxxi. Maji, Swarup Kumar, Nillohit Mukherjee, Amit Kumar Dutta, Divesh N Srivastava, Parimal Paul, Basudeb Karmakar, Anup Mondal, and Bibhutoh Adhikary. 2011. "Deposition of Nanocrystalline CuS Thin Film from a Single Precursor: Structural, Optical and Electrical Properties." *Materials Chemistry and Physics* 130 (1–2): 392–97.
- xxxii. Mohammadzadeh Jahani, Peyman, Hamid Akbari Javar, and Hadi Mahmoudi-Moghaddam. 2020. "Development of a Novel Electrochemical Sensor Using the FeNi₃/CuS/BiOCl Nanocomposite for Determination of Naproxen." *Journal of Materials Science: Materials in Electronics* 31 (17): 14022–34. <https://doi.org/10.1007/s10854-020-03876-9>.
- xxxiii. Morina, Naim, Gëzim Boçari, Ali Iljazi, Kadir Hyseini, and Gunay Halac. 2016. "Maximum Time of the Effect of Antileukotriene-Zileuton in Treatment of Patients with Bronchial Asthma." *Acta Informatica Medica* 24 (1): 16.
- xxxiv. Nabil A. Alhemiary., Moustafa. A . Rizk. 2017. "Sensitive and Validated Voltametric Methods for Determination of Zileuton in Serum, Urine and Pharmaceutical Dosage Forms at Activated Glassy Carbon Electrode." *Asian J Chem* 29 (12): 2627–33. <https://doi.org/https://doi.org/10.14233/ajchem.2017.20737>.
- xxxv. Naghian, Ebrahim, and Mostafa Najafi. 2018. "Carbon Paste Electrodes Modified with SnO₂/CuS, SnO₂/SnS and Cu@SnO₂/SnS Nanocomposites as Voltammetric Sensors for Paracetamol and Hydroquinone." *Microchimica Acta* 185 (9). <https://doi.org/10.1007/S00604-018-2948-6>.
- xxxvi. Pian, P (1), E (1) Labovitz, K (1) Hoffman, C F (1) Clavijo, R (1) Rzasalynn, J L (1) Galinkin (2), U (1) Christians, A A (3) Vinks (5), and P (4) Malik (5). 2013. "Quantification of the 5-Lipoxygenase Inhibitor Zileuton in Human Plasma Using High Performance Liquid Chromatography-Tandem Mass Spectrometry." *Journal of Chromatography B: Analytical Technologies in the Biomedical and Life Sciences* 937 (October): 79–83. <https://doi.org/10.1016/j.jchromb.2013.08.014>.
- xxxvii. PRAKASH, Katakam, Shanta K ADIKI, and Rama Rao KALAKUNTALA. 2014. "Development and Validation of a Liquid Chromatography-Mass Spectrometry Method for the Determination of Zileuton in Human Plasma." *Scientia Pharmaceutica* 82 (3): 571–83. <http://10.0.14.213/scipharm.1402-19>.
- xxxviii. Qian, N X, X Zhang, X Sun, M Wang, X Y Sun, C Liu, R Rao, and Y Q Ma. 2020. "A Facile Method to Tune the Crystal Lattice/Morphology/Electronic State/Photocatalytic Performance of BiOCl." *Journal of Alloys and Compounds* 815: 152490.
- xxxix. Rao, K V, M Tanuja, Y SRINIVASA Rao, and T HEMANT Kumar. 2015. "Development and Validation of Spectrophotometric Methods for Estimation of Zileuton in Bulk and Its Dosage Form." *International Journal Chemical Sciences* 13 (2):

- 714–24.
- xl. Sakamoto, T, H Sunamura, H Kawaura, T Hasegawa, T Nakayama, and M Aono. 2003. “Nanometer-Scale Switches Using Copper Sulfide.” *Applied Physics Letters* 82 (18): 3032–34.
- xli. Saranya, M, and dan A Nirmala Grace. 2012. “Hydrothermal Synthesis of CuS Nanostructures with Different Morphology.” In *Journal of Nano Research*, 18:43–51. Trans Tech Publ.
- xlii. Shuai, Xuemin, Wenzhong Shen, Xiaoting Li, Zhaoyang Hou, Sanmin Ke, Gang Shi, Chunlong Xu, and Donghua Fan. 2018. “Cation Exchange Synthesis of CuS Nanotubes Composed of Nanoparticles as Low-Cost Counter Electrodes for Dye-Sensitized Solar Cells.” *Materials Science and Engineering: B* 227: 74–79.
- xliii. Sorkness, Christine A. 1997. “The Use of 5-lipoxygenase Inhibitors and Leukotriene Receptor Antagonists in the Treatment of Chronic Asthma.” *Pharmacotherapy: The Journal of Human Pharmacology and Drug Therapy* 17 (1P2): 50S-54S.
- xliv. Sreedhar, N Y, M Sankara Nayak, K Srinivasa Prasad, P R Prasad, and C Nageswar Reddy. 2010. “Electrochemical Reduction Behaviour of Zileuton at a Dropping Mercury Electrode by Polarography.” *E-Journal of Chemistry* 7 (1): 166–70.
- xlv. Sun, X, M Wang, N X Qian, X Y Sun, C Liu, X Zhang, R Rao, and Y Q Ma. 2019. “Ultra-Fine BiOCl Nanoparticles: Unprecedented Synthesis and Rich Surface-Dependent Properties.” *Applied Surface Science* 489: 1030–41.
- xlvi. Tajik, Somayeh, Hadi Beitollahi, Fariba Garkani Nejad, Mohadeseh Safaei, Kaiqiang Zhang, Quyet Van Le, Rajender S Varma, Ho Won Jang, and Mohammadreza Shokouhimehr. 2020. “Developments and Applications of Nanomaterial-Based Carbon Paste Electrodes.” *RSC Advances* 10 (36): 21561–81.
- xlvii. Wang, Xiufang, Hanmei Hu, Shaohua Chen, Kehua Zhang, Jun Zhang, Wensheng Zou, and Runxia Wang. 2015. “One-Step Fabrication of BiOCl/CuS Heterojunction Photocatalysts with Enhanced Visible-Light Responsive Activity.” *Materials Chemistry and Physics* 158: 67–73.
- xlviii. You, Dahea, Lascelles E Lyn-Cook Jr, Daniel M Gatti, Natalie Bell, Philip R Mayeux, Laura P James, William B Mattes, Gary J Larson, and Alison H Harrill. 2020. “Nitrosative Stress and Lipid Homeostasis as a Mechanism for Zileuton Hepatotoxicity and Resistance in Genetically Sensitive Mice.” *Toxicological Sciences* 175 (2): 220–35.
- xlix. Yuan, K D, J J Wu, M L Liu, L L Zhang, F F Xu, L D Chen, and F Q Huang. 2008. “Fabrication and Microstructure of P-Type Transparent Conducting CuS Thin Film and Its Application in Dye-Sensitized Solar Cell.” *Applied Physics Letters* 93 (13): 132106.